# Experimental Validation of a Constrained Relative Attitude Determination Approach for Two Vehicle Formations

John McGreevy,[*] Joanna Hinks,[†] Richard Linares,[‡] John L. Crassidis[§]

*University at Buffalo, State University of New York, Amherst, NY, 14260-4400*

**This paper presents an experimental validation of a method of determining the relative attitude matrix between two quadrotors using line-of-sight vectors between each other as well as a common reference location. The result of the line-of-sight vector method is compared to the relative attitude matrix obtained from a motion capture system which is taken as the ground truth. The difference between the two measurements is calculated and then analyzed to characterize the error that occurs in the sensor model.**

## I. Introduction

There are many applications that require knowing the relative attitude of two or more vehicles. Knowing the relative attitude may be important whenever communication or cooperation between different vehicles is necessary. For instance, relative orientation of antennas might affect radio signals, or relative vehicle orientation might determine the success or failure of a transfer of items between different vehicles. Such applications may occur for unmanned aerial vehicles (UAVs) as well as for spacecraft formations.

For UAV formations to be effective, they must be able to maintain their formation, reconfigure to new formations as required, and also avoid collisions with either each other or with other obstacles.[1] Another application of relative attitude determination is performing inspections between two satellites.[2] For this situation, the instrumentation on the observing satellite must be oriented towards the observed satellite, and the relative orientation of the observed satellite must be known as well to ensure that the area of interest on the observed satellite is in the field of view of the observing satellite. The Global Positioning System (GPS) can be used to determine the relative attitude between two vehicles; however GPS is subject to several limitations. First, GPS measurements can only initially obtain the attitude relative to an inertial frame. This must then be converted to the relative attitude matrix, costing both computational time and energy. Both computation and energy can be valuable resources on vehicles such as spacecraft. GPS systems also require the ability to observe multiple other reference points instead of just one reference point as well as also vulnerable to jamming which can reduce the accuracy or even prevent obtaining an attitude matrix.

Motion capture technology has been used for a quadrotor in flight.[3] By placing four markers on each vehicle for the motion capture system to track, the system is able to determine both the location and attitude of each vehicle relative to a common reference coordinate system. This information can then be compared to the data collected by each vehicle to verify the relative attitude matrix obtained by the vehicles.

The line-of-sight method between each vehicle has been proven to determine a unique solution.[4] However, this solution requires knowledge of the LOS vectors obtained by the other vehicle. The set of LOS vectors can then be used to calculate the relative attitude matrix between each vehicle without need of an intermediate inertial reference frame.

This paper presents an experimental verification of the relative attitude determination discussed in Ref. 5. Using line-of-sight (LOS) vectors, the relative attitude between two vehicles can be determined. Both

[*]Undergraduate Student, Department of Mechanical & Aerospace Engineering. Email: jjm58@buffalo.edu, Student Member AIAA.

[†]Postdoctoral Assistant, Department of Mechanical & Aerospace Engineering. Email: jchinks@buffalo.edu, Member, AIAA.

[‡]Graduate Student, Department of Mechanical & Aerospace Engineering. Email: linares2@buffalo.edu, Student Member AIAA.

[§]Professor, Department of Mechanical & Aerospace Engineering. Email: johnc@buffalo.edu, Associate Fellow AIAA.

vehicles, with the addition of a common reference point, form a triangle with each vehicle and the common reference point forming a separate vertex of the triangle. Two non-inertial LOS vectors are obtained for each vehicle, one to the other vehicle while the other vector is to the common reference point. The two angles located at the two vehicles in the triangle formed by this formation can be obtained from the LOS vectors, and these angles can be used to calculate the third angle of the triangle. The relative attitude matrix can be obtained by first obtaining a rotation to align the two LOS vectors between the vehicles and then applying a rotation to satisfy the constraint that the remaining vectors from each vehicle to the common reference point are located in a plane. This approach to relative attitude determination has been verified in simulation in Ref. 5. The present paper extends that work by applying the technique to real experimental data.

The experiment consists of two quadrotor helicopters representing the vehicles. The helicopters have six infrared cameras mounted facing different directions to pick up the infrared LEDs mounted to each helicopter. The resulting attitude matrix obtained from the algorithm in Ref. 5 will be compared to the attitude matrix given by the VICON motion capture system.[6]

## II. Configuration and Sensor Model

Figure 1 shows the configuration and observations used for the solution of the relative attitude from frame $\mathcal{B}_1$ to frame $\mathcal{B}_2$. The vector $\mathbf{w}_1$ is the LOS observation from $\mathcal{B}_2$ to $\mathcal{B}_1$ expressed in $\mathcal{B}_2$ coordinates. The

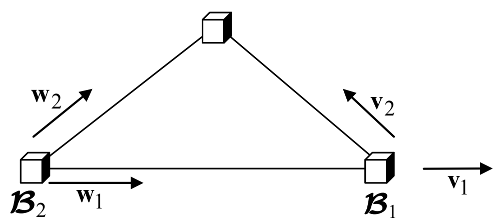


**Figure 1. Observation Geometry**

vector $\mathbf{v}_1$ is the LOS observation from $\mathcal{B}_2$ to $\mathcal{B}_1$ expressed in $\mathcal{B}_1$ coordinates; note, in practice the negative of this vector is measured. The vector $\mathbf{w}_2$ is the LOS observation from $\mathcal{B}_2$ to the common object expressed in $\mathcal{B}_2$ coordinates. Finally, the vector $\mathbf{v}_2$ is the LOS observation from $\mathcal{B}_1$ to the common object expressed in $\mathcal{B}_1$ coordinates.

Line-of-sight unit vector observations are typically obtained indirectly. A camera measures the 2-dimensional position of an incident light beam on a focal plane, and then uses a mathematical model to compute the LOS vector. The resulting unit vector, $\tilde{\mathbf{b}}$, can be approximated as a measurement with additive noise given by

$$\tilde{\mathbf{b}} = \mathbf{b} + \boldsymbol{\upsilon} \tag{1}$$

with

$$\boldsymbol{\upsilon} \sim \mathcal{N}(\mathbf{0}, \boldsymbol{\Omega}) \tag{2}$$

where $\boldsymbol{\upsilon}$ is assumed to be a Gaussian random vector with zero mean and covariance $\Omega$. As the constructed measurement $\tilde{\mathbf{b}}$ is constrained to have unit length, the noise $\boldsymbol{\upsilon}$ must be orthogonal to the true LOS vector and its covariance will be singular. The calculation for the covariance $\Omega$ depends on the assumptions made about the camera sensor and the camera's mathematical model. Two methods for calculating $\Omega$ are the standard QUEST measurement model[7] and an adapted model for sensors with a wide field of view (FOV).[8] For the present experiment, however, a covariance has been computed directly from an empirically-derived model for the quadrotor camera measurements. The reminder of this section briefly describes the QUEST and wide FOV models, and then presents a more detailed outline of the quadrotor camera model and the associated covariance calculations.

The raw measurement can be expressed as coordinates in the focal plane, denoted by $\alpha$ and $\beta$. The focal plane coordinates can be written in a $2 \times 1$ vector $\mathbf{m} \equiv [\alpha \quad \beta]^T$ with the measurement model

$$\tilde{\mathbf{m}} = \mathbf{m} + \mathbf{w} \tag{3}$$

A typical model for the noise $\mathbf{w}$ in the focal-plane coordinate observations for many camera systems is given as:[9]

$$\mathbf{w} \sim \mathcal{N}\left(\mathbf{0}, R^{\text{FOCAL}}\right) \tag{4a}$$

$$R^{\text{FOCAL}} = \frac{\sigma^2}{1 + d\left(\alpha^2 + \beta^2\right)} \begin{bmatrix} \left(1 + d\alpha^2\right)^2 & \left(d\alpha\beta\right)^2 \\ \left(d\alpha\beta\right)^2 & \left(1 + d\beta^2\right)^2 \end{bmatrix} \tag{4b}$$

where $\sigma^2$ is the variance of the measurement errors associated with $\alpha$ and $\beta$, and $d$ is on the order of 1. The covariance $R^{\text{FOCAL}}$ for the focal plane measurements is a function of the true values and this covariance realistically increases as the distance from the boresight increases. One example system that can be modeled by Eq. (4) is the vision-based navigation system.[10] This system has a position sending diode as the focal plane, and it captures incident light from a beacon emitted from a neighboring vehicle. This sensor has the advantage of having a small size and a very wide FOV.[11]

A general unit-length LOS observation can be expressed in terms of the focal plane coordinates as

$$\mathbf{b} = \frac{1}{\sqrt{f^2 + \alpha^2 + \beta^2}} \begin{bmatrix} \alpha \\ \beta \\ f \end{bmatrix} \tag{5}$$

where $f$ denotes the focal length. Shuster[7] has shown that the probability density for unit vector measurements lies on a sphere and can accurately be approximated by a density on a plane tangent to the vector for sensors with a sufficiently small FOV. This approximation is known as the QUEST measurement model. It characterizes $\boldsymbol{\upsilon}$, the LOS additive noise process resulting from the focal plane model of Eq. (4), as a zero-mean Gaussian vector with covariance

$$\Omega \equiv E\left\{\boldsymbol{\upsilon}\boldsymbol{\upsilon}^T\right\} = \sigma^2\left(I_{3\times 3} - \mathbf{b}\mathbf{b}^T\right) \tag{6}$$

The covariance of Eq. (6) is only valid for a small FOV, for which a tangent plane closely approximates the surface of a unit sphere. For wide-FOV sensors, a more accurate measurement covariance is shown in Ref. 8. This formulation employs a first-order Taylor series approximation about the focal-plane axes. The partial derivative operator is used to linearly expand the focal-plane covariance in Eq. (4), given by

$$J = \frac{\partial \mathbf{b}}{\partial \mathbf{m}} = \frac{1}{\sqrt{1 + \alpha^2 + \beta^2}} \begin{bmatrix} 1 & 0 \\ 0 & 1 \\ 0 & 0 \end{bmatrix} - \frac{1}{1 + \alpha^2 + \beta^2} \mathbf{b}\mathbf{m}^T \tag{7}$$

where a focal length of $f = 1$ has been assumed. Then the wide-FOV covariance model is given by

$$\Omega = J\, R^{\text{FOCAL}} J^T \tag{8}$$

If a camera with a small FOV is used, then Eq. (8) is still valid, but it is nearly identical to Eq. (6).

For the present experiment, the quadrotor cameras are PixArt infrared cameras taken from a Nintendo Wii remote. More details about the experimental setup are provided in Section IV. The camera has a field of view of $\pm 20$ degrees in the horizontal direction and $\pm 15$ degrees in the vertical direction. Each quadrotor carries three cameras oriented outward and orthogonal to each other. The raw focal plane measurements from these cameras are assumed to take the form of Eq. (3), where the zero-mean noise $\mathbf{w}$ has covariance

$$\mathbf{w} = \begin{bmatrix} \delta\alpha \\ \delta\beta \end{bmatrix} \sim \begin{bmatrix} \sigma_\alpha^2 & 0 \\ 0 & \sigma_\beta^2 \end{bmatrix} \tag{9}$$

From each focal plane observation pair $(\alpha, \beta)$, a unit vector is constructed in spherical coordinates. The spherical coordinate angles $\theta$ and $\phi$ are related to $\alpha$ and $\beta$ by the functions

$$\theta\left(\alpha, \beta\right) = p_{00} + p_{10}\alpha + p_{01}\beta \tag{10a}$$

$$\phi\left(\alpha, \beta\right) = q_{00} + q_{10}\alpha + q_{01}\beta \tag{10b}$$

In these equations, the scalar coefficients $p_{ij}$ and $q_{ij}$ have been empirically measured for each individual camera, along with standard deviations for these measurements. The assumed measurement models for these coefficients are given by

$$\tilde{p}_{ij} = p_{ij} + \delta p_{ij}, \qquad \delta p_{ij} \sim \mathcal{N}\left(0, \sigma_{pij}^2\right) \tag{11a}$$

$$\tilde{q}_{ij} = q_{ij} + \delta q_{ij}, \qquad \delta q_{ij} \sim \mathcal{N}\left(0, \sigma_{qij}^2\right) \tag{11b}$$

Finally, the unit vector $\mathbf{b}$ is constructed from the angles $\theta$ and $\phi$ as

$$\mathbf{b} = \begin{bmatrix} \cos\theta\cos\phi \\ \cos\theta\sin\phi \\ \sin\theta \end{bmatrix} \tag{12}$$

Depending on the orientation of a particular camera on the quadrotor, an additional 90-degree rotation of the vector in Eq. (12) may be necessary, but this only causes a permutation of the elements.

The covariance of the noise $\boldsymbol{\upsilon}$ in the unit vector measurement $\tilde{\mathbf{b}}$ is obtained for this camera model by propagating uncertainties through the equations and taking expectations. For simplicity, the noise terms are assumed to be small relative to the measurements, and small-angle approximations are incorporated. First, the means, covariances, and cross-covariances of $\theta$ and $\phi$ are obtained by substituting $(\alpha + \delta\alpha)$, $(\beta + \delta\beta)$, $(p_{ij} + \delta p_{ij})$, and $(q_{ij} + \delta q_{ij})$ into Eqs. (10a) and (10b) and taking expectations. The resulting expressions for $\theta$ and $\phi$ can be written in a manner analogous to measurement functions:

$$\begin{bmatrix} \tilde{\theta} \\ \tilde{\phi} \end{bmatrix} = \begin{bmatrix} \theta \\ \phi \end{bmatrix} + \begin{bmatrix} \delta\theta \\ \delta\phi \end{bmatrix} \tag{13}$$

where $\delta\theta$ and $\delta\phi$ are zero-mean with covariance

$$\mathrm{E}\left\{ \begin{bmatrix} \delta\theta \\ \delta\phi \end{bmatrix} \begin{bmatrix} \delta\theta & \delta\phi \end{bmatrix} \right\} = \begin{bmatrix} \sigma_\theta^2 & \sigma_{\theta\phi} \\ \sigma_{\theta\phi} & \sigma_\phi^2 \end{bmatrix} \tag{14}$$

and

$$\sigma_\theta^2 = \sigma_{p00}^2 + p_{10}^2\sigma_\alpha^2 + p_{01}^2\sigma_\beta^2 + \alpha^2\sigma_{p10}^2 + \beta^2\sigma_{p01}^2 \tag{15a}$$

$$\sigma_\phi^2 = \sigma_{q00}^2 + q_{10}^2\sigma_\alpha^2 + q_{01}^2\sigma_\beta^2 + \alpha^2\sigma_{q10}^2 + \beta^2\sigma_{q01}^2 \tag{15b}$$

$$\sigma_{\theta\phi} = p_{10}q_{10}\sigma_\alpha^2 + p_{01}q_{01}\sigma_\beta^2 \tag{15c}$$

Next, Eq. (13) is substituted into the unit vector equation, Eq. (12), and expectation operations are performed once more to compute the LOS vector covariance $\Omega$. After much algebra and appropriate small-angle approximations, the final expression for covariance is

$$\Omega = \mathrm{E}\left[\left(\tilde{\mathbf{b}} - \mathbf{b}\right)\left(\tilde{\mathbf{b}} - \mathbf{b}\right)^T\right] = \begin{bmatrix} \Omega_{11} & \Omega_{12} & \Omega_{13} \\ \Omega_{12} & \Omega_{22} & \Omega_{23} \\ \Omega_{13} & \Omega_{23} & \Omega_{33} \end{bmatrix} \tag{16}$$

where the six unique elements of the matrix $\Omega$ are given by

$$\begin{aligned} \Omega_{11} &= \sin^2\theta\cos^2\phi\,\sigma_\theta^2 + \cos^2\theta\sin^2\phi\,\sigma_\phi^2 + 2\cos\theta\sin\theta\cos\phi\sin\phi\,\sigma_{\theta\phi} \\ &\quad + \sin^2\theta\sin^2\phi\left(3p_{10}^2q_{10}^2\sigma_\alpha^4 + 3p_{01}^2q_{01}^2\sigma_\beta^4 - \sigma_{\theta\phi}^2\right) \end{aligned} \tag{17a}$$

$$\begin{aligned} \Omega_{22} &= \sin^2\theta\sin^2\phi\,\sigma_\theta^2 + \cos^2\theta\cos^2\phi\,\sigma_\phi^2 - 2\cos\theta\sin\theta\cos\phi\sin\phi\,\sigma_{\theta\phi} \\ &\quad + \sin^2\theta\cos^2\phi\left(3p_{10}^2q_{10}^2\sigma_\alpha^4 + 3p_{01}^2q_{01}^2\sigma_\beta^4 + 3\sigma_{\theta\phi}^2\right) \end{aligned} \tag{17b}$$

$$\Omega_{33} = \cos^2\theta\,\sigma_\theta^2 \tag{17c}$$

$$\begin{aligned} \Omega_{12} &= \sin^2\theta\cos\phi\sin\phi\,\sigma_\theta^2 - \cos^2\theta\cos\phi\sin\phi\,\sigma_\phi^2 + \cos\theta\sin\theta\left(\sin^2\phi - \cos^2\phi\right)\sigma_{\theta\phi} \\ &\quad - \sin^2\theta\cos\phi\sin\phi\left(3p_{10}^2q_{10}^2\sigma_\alpha^4 + 3p_{01}^2q_{01}^2\sigma_\beta^4 - \sigma_{\theta\phi}^2\right) \end{aligned} \tag{17d}$$

$$\Omega_{13} = -\sin\theta\cos\theta\cos\phi\,\sigma_\theta^2 - \cos^2\theta\sin\phi\,\sigma_{\theta\phi} \tag{17e}$$

$$\Omega_{23} = -\cos\theta\sin\theta\sin\phi\,\sigma_\theta^2 + \cos^2\theta\cos\phi\,\sigma_{\theta\phi} \tag{17f}$$

All three LOS vector measurement models (QUEST, wide FOV, and the model based on this experiment's camera) yield a singular $3\times 3$ covariance $\Omega$ because the unit-length LOS vectors have only two independent parameters. A nonsingular covariance matrix for the LOS measurements can be obtained for all three methods by a rank-one update to $\Omega$:

$$\Omega_{\text{new}} = \Omega + \frac{1}{2}\text{trace}\,(\Omega)\,\mathbf{b}\mathbf{b}^T \tag{18}$$

which can be used without loss in generality to develop attitude-error covariance expressions.[12] The computed covariances are for the LOS measurements in the body frame corresponding to that particular quadrotor. The four measurements and their respective covariances, using notation defined by Fig. 1 instead of $\mathbf{b}$, are summarized by

$$\tilde{\mathbf{w}}_1 = \mathbf{w}_1 + \boldsymbol{\upsilon}_{w1}, \quad \boldsymbol{\upsilon}_{w1} \sim \mathcal{N}\left(\mathbf{0}, R_{w_1}\right) \tag{19a}$$
$$\tilde{\mathbf{w}}_2 = \mathbf{w}_2 + \boldsymbol{\upsilon}_{w2}, \quad \boldsymbol{\upsilon}_{w2} \sim \mathcal{N}\left(\mathbf{0}, R_{w_2}\right) \tag{19b}$$
$$\tilde{\mathbf{v}}_1 = \mathbf{v}_1 + \boldsymbol{\upsilon}_{v1}, \quad \boldsymbol{\upsilon}_{v1} \sim \mathcal{N}\left(\mathbf{0}, R_{v_1}\right) \tag{19c}$$
$$\tilde{\mathbf{v}}_2 = \mathbf{v}_2 + \boldsymbol{\upsilon}_{v2}, \quad \boldsymbol{\upsilon}_{v2} \sim \mathcal{N}\left(\mathbf{0}, R_{v_2}\right) \tag{19d}$$

Since in practice each vehicle will have its own set of LOS measurement devices, the measurements in Eq. (19) can be assumed to be uncorrelated.

## III. Constrained Solution

This section summarizes the constrained attitude solution of Ref. 5. More details can be found in that reference. Considering the measurements shown in Fig. 1, to determine the full attitude between the $\mathcal{B}_2$ and $\mathcal{B}_1$ frames the attitude matrix must satisfy the following measurement equations:

$$\mathbf{w}_1 = A\mathbf{v}_1 \tag{20a}$$
$$d = \mathbf{w}_2^T A\mathbf{v}_2 \tag{20b}$$

It is assumed that $|d| \leq 1$; otherwise a solution will not exist. Also, it is assumed that the LOS vectors $\mathbf{v}_1$ and $\mathbf{w}_1$ are parallel. Also note that from Fig. 1 no observation information is required from the third object to either $\mathcal{B}_1$ or $\mathcal{B}_2$. Hence, no information such as position is required for this object to determine the relative attitude. A solution for the attitude satisfying Eq. (20) is discussed in Ref. 13 and will be utilized to form a solution for the constrained problem discussed here. The solution for the rotation matrix that satisfies Eq. (20) can be found by first finding a rotation matrix that satisfies the first equation and then finding the angle that one must rotate about the reference direction to align the two remaining vectors such that their dot product is equivalent to that measured in the remaining frame in the formation. The first rotation can be found by rotating about any direction by any angle, where $B = R\left(\mathbf{n}_1, \theta\right)$ is a general rotation about some axis that satisfies Eq. (20a). The choice of the initial rotation axis is arbitrary. Here, the vector that bisects the angle between the two reference direction vectors is used and the rotation is as follows:

$$B = \frac{(\mathbf{w}_1 + \mathbf{v}_1)(\mathbf{w}_1 + \mathbf{v}_1)^T}{(1 + \mathbf{v}_1^T\mathbf{w}_1)} - I_{3\times 3} \tag{21}$$

where $\mathbf{n}_1 = (\mathbf{w}_1 + \mathbf{v}_1)$ and $\theta = \pi$. This rotation matrix will align the LOS vectors $\mathbf{w}_1$ and $\mathbf{v}_1$ between frames, but the frames could still have some rotation about this vector, so the rotation about the $\mathbf{w}_1$ axis must be determined to solve the second equation. To do so the vector $\mathbf{w}^*$ is first defined, which is the vector produced after applying the rotation $B$ on the vector $\mathbf{v}_2$. This will allow us to determine the second rotation needed to map $\mathbf{v}_2$ properly to the $\mathcal{B}_2$ frame with $\mathbf{w}^* = B\,\mathbf{v}_2$. Since the rotation axis is the $\mathbf{w}_1$ vector, $\mathbf{w}_1$ will be invariant under this transformation and the solution to the full attitude can be written as $A = R\left(\mathbf{n}_2, \theta\right) B$.

Consider solving for the rotation angle using the planar constraint. The constraint can be written as:

$$0 = \mathbf{w}_2^T [\mathbf{w}_1 \times] R\left(\mathbf{n}_2, \theta\right) \mathbf{w}^* \tag{22}$$

where $[\mathbf{w}_1\times]$ denotes the cross product matrix for the vector $\mathbf{w}_1$. The definition of this matrix for a general $3\times 1$ vector $\boldsymbol{\alpha}$ is

$$[\boldsymbol{\alpha}\times] = \begin{bmatrix} 0 & -\alpha_3 & \alpha_2 \\ \alpha_3 & 0 & -\alpha_1 \\ -\alpha_2 & \alpha_1 & 0 \end{bmatrix} \tag{23}$$

Substituting the second rotation matrix into Eq. (22), and with $\mathbf{n}_2 = \mathbf{w}_1$, leads to

$$0 = \mathbf{w}_2^T[\mathbf{w}_1\times]\left(\mathbf{w}_1\mathbf{w}_1^T - \cos(\theta)[\mathbf{w}_1\times]^2\mathbf{w}^* - \sin(\theta)[\mathbf{w}_1\times]\mathbf{w}^*\right) \tag{24}$$

Expanding out this expression yields

$$\left(\mathbf{w}_2^T[\mathbf{w}_1\times]\mathbf{w}^*\right)\cos(\theta) = \left(\mathbf{w}_2^T[\mathbf{w}_1\times]^2\mathbf{w}^*\right)\sin(\theta) \tag{25}$$

Notice that if Eq. (25) is divided by $-1$ then the equation would be unchanged but the solution for the angle $\theta$ would differ by $\pi$. Therefore, using the planar constraint the solution for the angle $\theta$ can be written as $\theta = \beta + \phi$, where

$$\beta = \text{atan2}(\mathbf{w}_2^T[\mathbf{w}_1\times]\mathbf{w}^*, \mathbf{w}_2^T[\mathbf{w}_1\times]^2\mathbf{w}^*) \tag{26}$$

and $\phi = 0$ or $\pi$. Note that these are not the same $\beta$, $\theta$ and $\phi$ used in the derivation for the measurement model covariance. An ambiguity exists when using this approach but it is important to note that one of the possible solutions for this approach is equivalent to the triangle constraint case.

Finally the solution for the attitude is given by $A = R(\mathbf{w}_1,\theta)\,B$. The solution is now summarized:

$$B = \frac{(\mathbf{w}_1+\mathbf{v}_1)(\mathbf{w}_1+\mathbf{v}_1)^T}{(1+\mathbf{v}_1^T\mathbf{w}_1)} - I_{3\times 3} \tag{27a}$$

$$R(\mathbf{w}_1,\theta) = I_{3\times 3}\cos(\theta) + (1-\cos(\theta))\mathbf{w}_1\mathbf{w}_1^T - \sin(\theta)[\mathbf{w}_1\times] \tag{27b}$$

$$\theta = \text{atan2}(\mathbf{w}_2^T[\mathbf{w}_1\times]\mathbf{w}^*, \mathbf{w}_2^T[\mathbf{w}_1\times]^2\mathbf{w}^*) + \pi \tag{27c}$$

$$A = R(\mathbf{w}_1,\theta)\,B \tag{27d}$$

This result shows that for any formation of two vehicles a deterministic solution will exist using one direction and one angle. Due to the fact that our case is truly deterministic there is no need to minimize a cost function and the solution will always be the maximum likelihood one. It is very important to note that without the resolution of the attitude ambiguity any covariance development might not have any meaning since although the covariance might take a small value if the wrong possible attitude is used then the error might be fairly large and not bounded by the attitude covariance.

The solution in Eq. (27) can be rewritten without the use of any transcendental functions. The following relationships can be derived:

$$\cos(\theta) = -\frac{\mathbf{w}_2^T[\mathbf{w}_1\times]^2\mathbf{w}^*}{\|\mathbf{w}_1\times\mathbf{w}_2\|\|\mathbf{v}_1\times\mathbf{v}_2\|} \tag{28a}$$

$$\sin(\theta) = -\frac{\mathbf{w}_2^T[\mathbf{w}_1\times]\mathbf{w}^*}{\|\mathbf{w}_1\times\mathbf{w}_2\|\|\mathbf{v}_1\times\mathbf{v}_2\|} \tag{28b}$$

This leads to $\cos(\theta) = -b/c$ and $\sin(\theta) = -a/c$ with

$$a = \mathbf{w}_2^T[\mathbf{w}_1\times]\left([\mathbf{w}_1\times] + [\mathbf{v}_1\times]\right)[\mathbf{v}_1\times]\mathbf{v}_2 \tag{29a}$$

$$b = \mathbf{w}_2^T[\mathbf{w}_1\times]\left([\mathbf{w}_1\times][\mathbf{v}_1\times] - I_{3\times 3}\right)[\mathbf{v}_1\times]\mathbf{v}_2 \tag{29b}$$

$$c = (1+\mathbf{v}_1^T\mathbf{w}_1)\|\mathbf{w}_1\times\mathbf{w}_2\|\|\mathbf{v}_1\times\mathbf{v}_2\| \tag{29c}$$

Note that $c = \sqrt{a^2+b^2}$. Then the matrix $R$ is given by

$$R = -\frac{b}{c}I_{3\times 3} + \left(1+\frac{b}{c}\right)\mathbf{w}_1\mathbf{w}_1^T + \frac{a}{c}[\mathbf{w}_1\times] \tag{30}$$

Noting that $\mathbf{w}_1\mathbf{w}_1^T B = \mathbf{w}_1\mathbf{v}_1^T$ then the solution in Eq. (27d) can be rewritten as

$$\begin{aligned} A = \frac{b}{c}\left(I_{3\times 3} - \frac{(\mathbf{w}_1+\mathbf{v}_1)(\mathbf{w}_1+\mathbf{v}_1)^T}{(1+\mathbf{v}_1^T\mathbf{w}_1)} + \mathbf{w}_1\mathbf{v}_1^T\right) \\ + \frac{a}{c}[\mathbf{w}_1\times]\left(\frac{\mathbf{v}_1\mathbf{w}_1^T+\mathbf{v}_1\mathbf{v}_1^T}{(1+\mathbf{v}_1^T\mathbf{w}_1)} - I_{3\times 3}\right) + \mathbf{w}_1\mathbf{v}_1^T \end{aligned} \tag{31}$$

Note in practice the measured quantities from the previous section are used in place of the observed quantities shown in Eq. (27), and Eqs. (29) and (31).

The covariance matrix for an attitude estimate is defined as the covariance of a small angle rotation taking the true attitude to the estimated attitude. Typically the small Euler angles are used to parameterize the attitude error-matrix. Reference 5 derives the attitude error-covariance for the constrained solution by using the attitude matrix with respect to the small angle errors. The attitude error-covariance is given by

$$P = \left(\begin{bmatrix} -[A_{\text{true}}\mathbf{v}_1\times] \\ -\mathbf{w}_2^T[\mathbf{w}_1\times][A_{\text{true}}\mathbf{v}_2\times] \end{bmatrix}^T \begin{bmatrix} R_{\Delta_1} & R_{\Delta_1\Delta_2} \\ R_{\Delta_1\Delta_2}^T & R_{\Delta_2} \end{bmatrix}^{-1} \begin{bmatrix} -[A_{\text{true}}\mathbf{v}_1\times] \\ -\mathbf{w}_2^T[\mathbf{w}_1\times][A_{\text{true}}\mathbf{v}_2\times] \end{bmatrix}\right)^{-1} \tag{32}$$

where

$$R_{\Delta_1} = R_{w_1} + A_{\text{true}}R_{v_1}A_{\text{true}}^T \tag{33a}$$

$$\begin{aligned} R_{\Delta_2} = -\big\{\mathbf{w}_2^T[A_{\text{true}}\mathbf{v}_2\times]R_{w_1}[A_{\text{true}}\mathbf{v}_2\times]\mathbf{w}_2 + (A_{\text{true}}\mathbf{v}_2)^T[\mathbf{w}_1\times]R_{w_2}[\mathbf{w}_1\times](A_{\text{true}}\mathbf{v}_2) \\ + \mathbf{w}_2^T[\mathbf{w}_1\times]A_{\text{true}}R_{v_2}A_{\text{true}}^T[\mathbf{w}_1\times]\mathbf{w}_2\big\} \end{aligned} \tag{33b}$$

$$R_{\Delta_1\Delta_2} = -R_{w_1}[A_{\text{true}}\mathbf{v}_2\times]\mathbf{w}_2 \tag{33c}$$

This expression is a function of the true attitude, $A_{\text{true}}$, but the true attitude can effectively be replaced with the estimated attitude to within first order.

# IV. Experiment

## A. Setup

The experiment consists of two remote-controlled quadrotor helicopters,[3] shown in Figs. 2 and 3. These

**Figure 2. Image of Quadrotors Used**

quadrotors are flown in the range of a Vicon motion capture system at the University at Buffalo (Fig. 4). The quadrotors have markers placed on the fuselage that can be detected by the Vicon system and resolve positions of each marker with an accuracy of 1 mm.[6] By placing at least 4 markers on each quadrotor, the

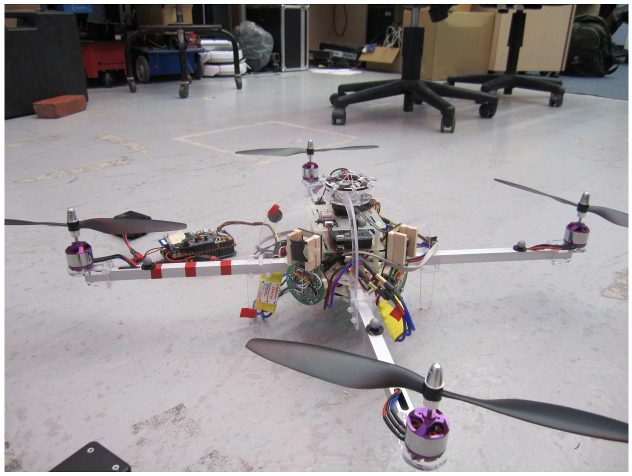

**Figure 3. Detailed View of Quadrotor with Cameras**

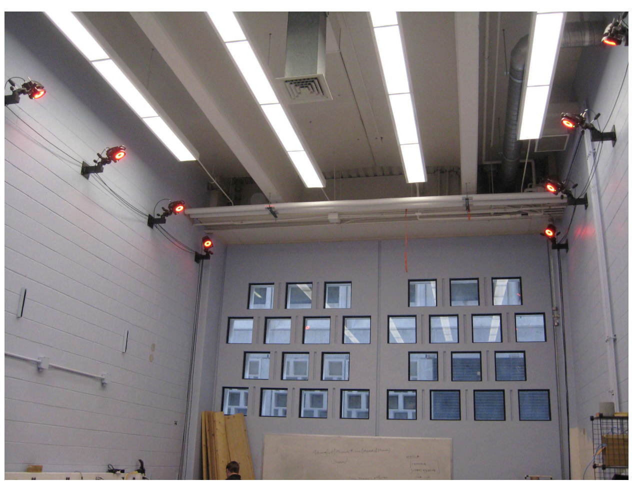

**Figure 4. Experimental Facility**

attitude with respect to the reference coordinate system of the Vicon system is determined and reported as 3-2-1 Euler angles. From the Euler angles, the attitude matrix from the Vicon coordinate system to each quadrotor body frame can be determined, and thus the relative attitude matrix from $\mathcal{B}_2$ to $\mathcal{B}_1$ can be determined.

Each camera being used is a PixArt infrared camera, as described in Section II. The camera has the ability to track up to 4 individual points simultaneously and is most sensitive to the 940 nm wavelength. Each quadrotor has infrared light emitting diodes (LEDs) with a wavelength of 940 nm located around the center of the body for the cameras on the other quadrotor to detect. There are also infrared LEDs located at the origin of the coordinate system used by the Vicon system as the common reference object. The LEDs located at the common reference object are arranged in a pattern that is distinguishable from the LEDs on the quadrotors as the infrared cameras used in this experiment are unable to distinguish between different wavelengths of light.

The camera data are read and processed by an Arduino Mega 2560 microcontroller. The microcontroller takes the position data of the LEDs detected by the cameras and converts the data into vector form. It computes one vector in the direction of the other quadrotor, and a second vector in the direction of the common reference point. The microcontroller in the $\mathcal{B}_1$ vehicle frame then communicates via Bluetooth to the other quadrotor to obtain the $\mathbf{w}_1$ and $\mathbf{w}_2$ vectors in the $\mathcal{B}_2$ vehicle frame and uses Eq. (27) to calculate the relative attitude matrix from $\mathcal{B}_2$ to $\mathcal{B}_1$.

### B. Calibration

The calibration for this setup is performed using the Vicon system to track the location of each quadrotor and the reference beacon. Asymmetric patterns of reflective markers are placed on each quadrotor and the reference beacon to allow Vicon to uniquely identify each object, as well as its position and orientation. The calibration is performed by placing the reference beacon at several different locations in the FOV of each camera and recording the pixel that detected the infrared LED, and the unit vector from the quadrotor to the reference beacon in the body frame of the quadrotor. The unit vector is converted to spherical coordinates, and a relationship between the two-dimensional Cartesian coordinates given by each camera and the spherical azimuth and elevation angles is fit. For these cameras, there is a linear relationship that transforms the camera coordinates into spherical coordinates in the body frame of the quadrotor.

### C. Procedure

To begin the experiment, the microcontrollers on each quadrotor are powered on and the Bluetooth communications between them are synchronized to share their vectors in real-time. Once the microcontrollers are synchronized and the Vicon data is being recorded, the quadrotors are moved around and rotated in the air with different attitudes relative to each other and different attitudes relative to their inertial surroundings. After sufficient data are obtained, recording is stopped, and the data from the Vicon system and from the onboard SD cards are uploaded to a computer and saved.

## V. Results & Discussion

The experiments conducted produced quaternion attitude solutions from both the Vicon system and the quadrotors. Figure 5 shows these two quaternion histories. Figure 6 shows the comparison between the Vicon system and the quadrotor quaternion elements individually. Note that the plot for element $\mathbf{q}_4$ has a different vertical scale from that of the other three elements, in order to more clearly show the variation. It is evident from these plots, particularly for the $q_2$ and $q_3$ quaternion elements, that there is a strong similarity between the Vicon and the quadrotor data. To determine the error between the two relative attitude matrices, the angle errors between the two attitudes are calculated and plotted in Fig. 7 along with their corresponding $3\sigma$ error bounds. The quadrotors are able to actively maintain LOS vectors between each other and the reference beacon throughout most of the experiment. These vectors are utilized to calculate the relative attitude between the two vehicles. As evidenced by the agreement between the quadrotor and Vicon data in the detailed plots for each quaternion component, the quadrotors are able to accurately obtain their relative attitudes. Figure 8 shows that the difference between the two attitudes is generally around 5 degrees or less, and rarely exceeded 10 degrees.

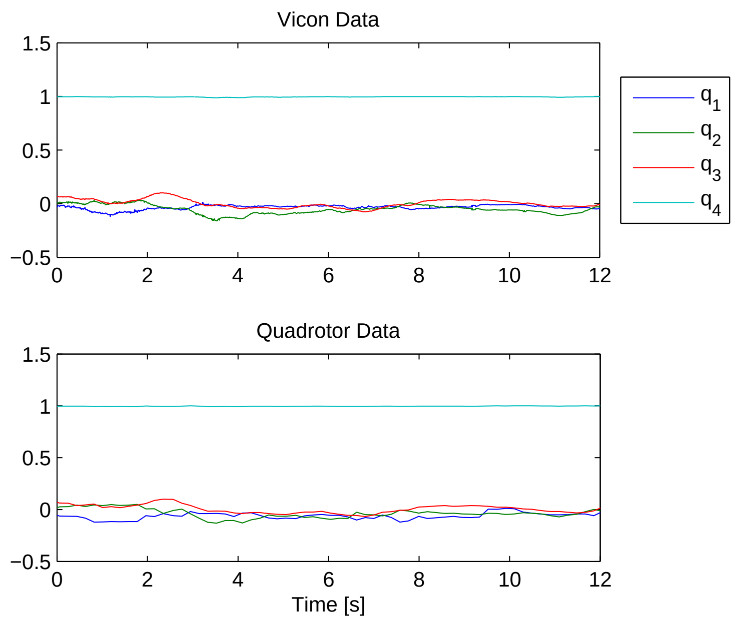


**Figure 5. Vicon and Quadrotor Quaternions**

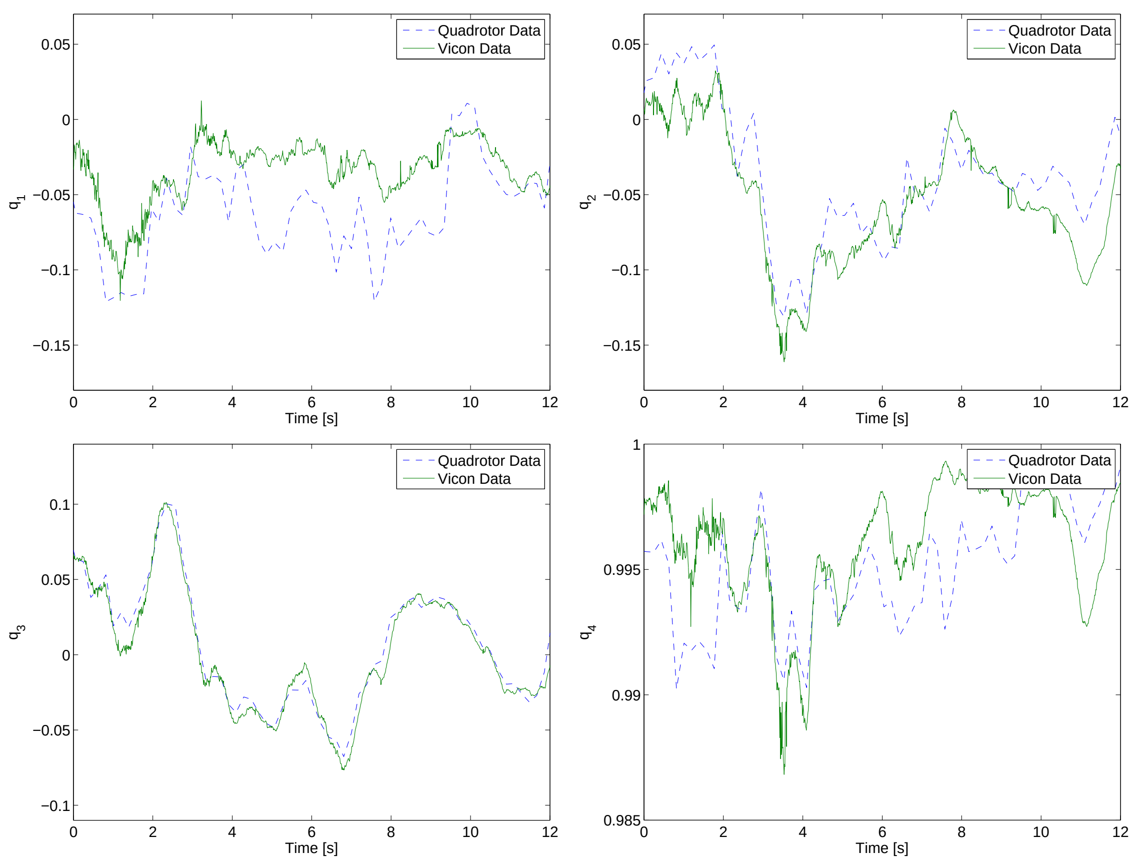


**Figure 6. Individual Quaternion Component Comparisons**

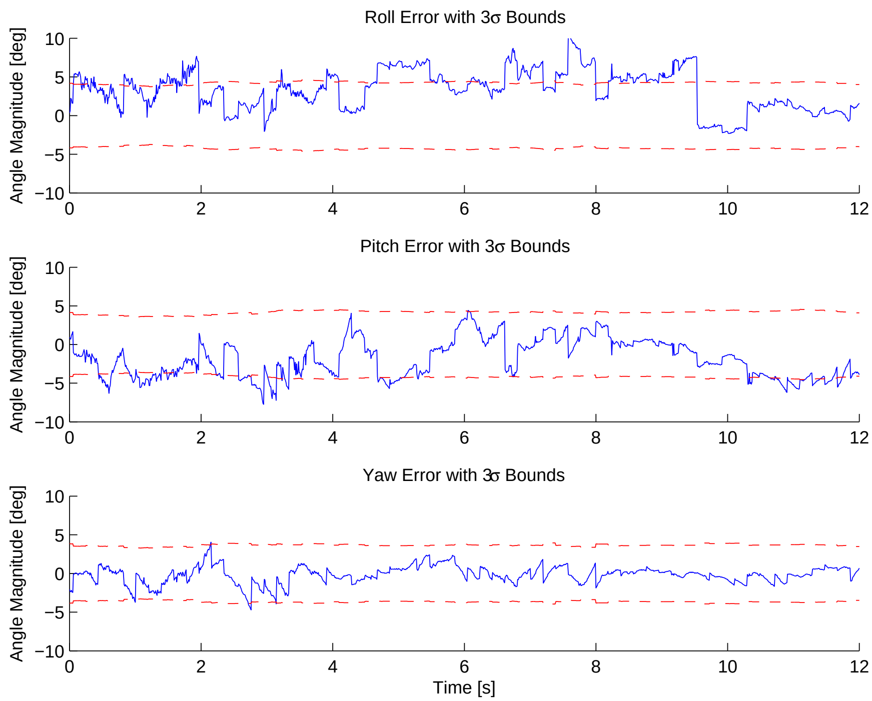


**Figure 7. Relative Attitude Measurement Errors**

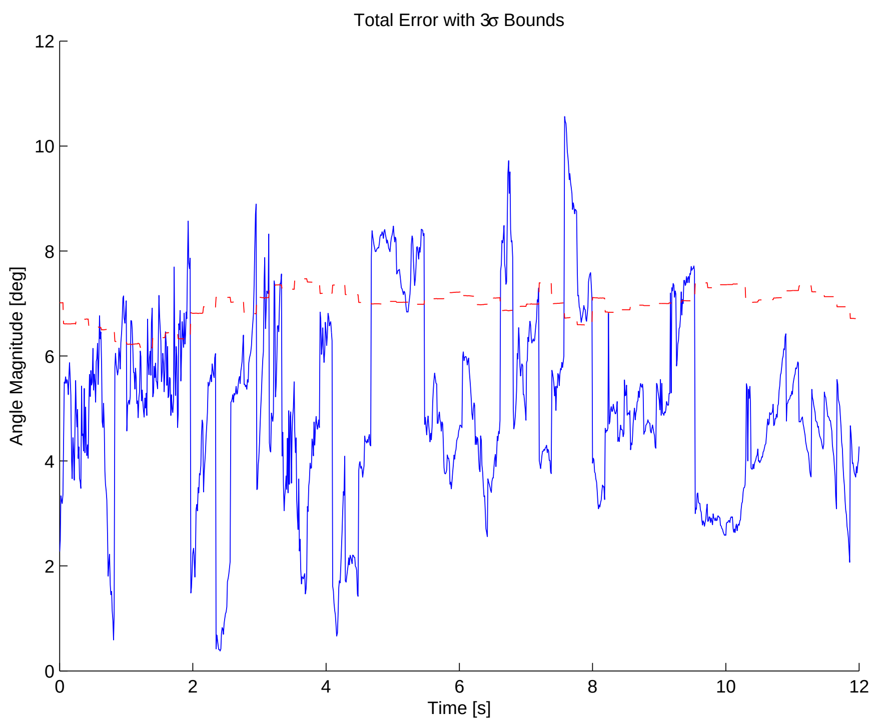


**Figure 8. Total Angular Error**

Some of the observed differences are caused by one of the cameras on the quadrotor failing to detect the infrared light source for a period of time. When this occurs, the quadrotor's reported attitude jumps sharply, resulting in a temporary divergence from the true attitude. An example of this failure occurs at around t=9 seconds in the $q_1$ component of the quaternion in Fig. 6.

In Figs. 7 and 8, the Vicon attitude solution is treated as the "truth" and the reported errors are relative to that solution. This treatment is reasonable because the Vicon measurements are known to have much greater accuracy than the quadrotor camera measurements. Another approach that accounts for the expected noise in both types of measurements is track-to-track correlation.[14] This technique tests the hypothesis that both estimated attitudes refer to the same underlying true attitude. One computes the statistic

$$y = \boldsymbol{\delta\alpha}^T \left(P_{11} + P_{22} - P_{12} - P_{21}\right)^{-1} \boldsymbol{\delta\alpha} \tag{34}$$

where $\boldsymbol{\delta\alpha}$ is the difference between the two estimates (in this case the vector of relative angles between the two attitudes). The matrices $P_{11}$ and $P_{22}$ are the covariances matrices associated with the estimation errors for each method, and the matrices $P_{12}$ and $P_{21}$ are their cross-covariances. If the Vicon and quadrotor solutions are in agreement, the computed test statistic should behave as a chi-squared random variable with three degrees of freedom, and 95% of the points should fall within the boundaries for such a distribution.

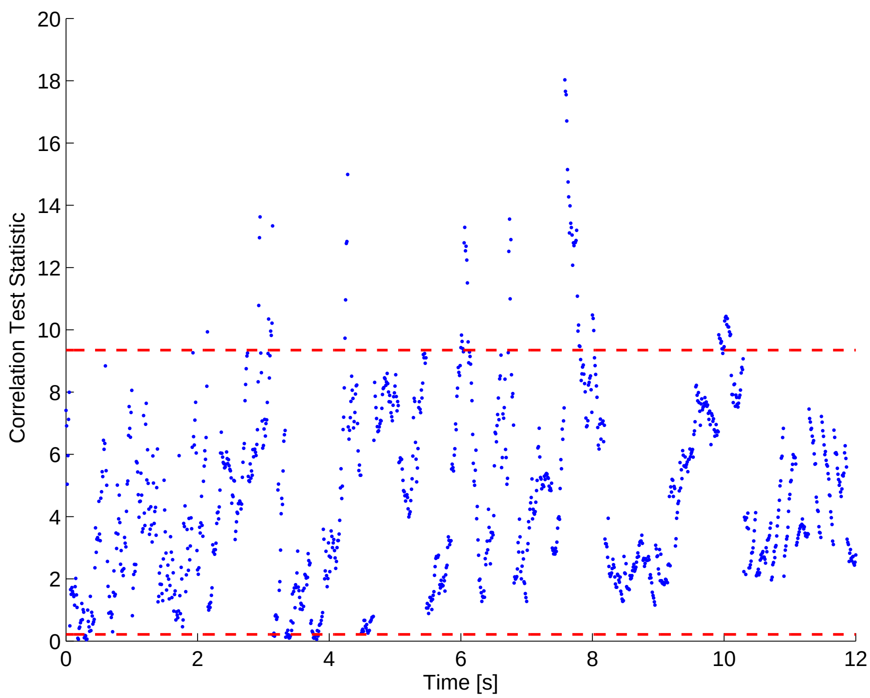


**Figure 9. Track-to-Track Correlation Statistic**

Figure 9 shows the correlation test statistic for the current experiment, along with the appropriate 95% bounds. For simplicity, the measurements from the two attitude sensors are assumed to be independent, such that $P_{12}$ and $P_{21}$ are zero. This assumption of independence is invalid for filtering methods which rely on the same underlying process noise, but it may be acceptable for point solutions such as those in the present experiment. A standard deviation of 1 degree is assumed for the Vicon attitude, and the covariance from the LOS vectors was computed using Eq. (32). The constant bias is also removed from each component of the attitude angle difference to account for poor calibration of the Vicon. The test statistic fell within the 95% bounds about 92% of the time, which indicates good agreement.

## VI. Conclusions

In this paper experimental verification of a relative attitude determination approach for two vehicles using a triangle constraint in the observations was presented. The triangle constraint is useful because it requires two fewer observations than a deterministic relative approach without the constraint. In actual practice, the triangle scenario reflects a realistic physical situation; however, out-of-plane deflections can occur due to misalignments and/or noise. This paper studied the practical implementation for the relative attitude determination approach using formation of two vehicles. A Vicon motion capture system was used to provide a more accurate alternative solution, and this solution was compared to the experimental data from two quadrotors. These two attitude solutions were compared statistically, and their strong agreement validated the proposed theory.

## References


[1] Ryan, A., Zennaro, M., Howell, A., Sengupta, R., and Hedrick, J. K., "An Overview of Emerging Results in Cooperative UAV Control," *43rd IEEE Conf. on Decision and Control*, Vol. 1, Dec. 2004, pp. 602–607.

[2] Horri, N. M., Kristiansen, K. U., Palmer, P., and Roberts, M., "Relative Attitude Dynamics and Control for a Satellite Inspection Mission," *Acta Astronautica*, Vol. 71, No. 0, 2012, pp. 109–118.

[3] Ducard, G. and D'Andrea, R., "Autonomous Quadrotor Flight using a Vision System and Accommodating Frames Misalignment," *IEEE Intl. Symposium on Industrial Embedded Systems*, July 2009, pp. 261–264.

[4] Andrle, M. S., Crassidis, J. L., Linares, R., and Cheng, Y., "Deterministic Relative Attitude Determination of Three-Vehicle Formations," *Journal of Guidance, Control, And Dynamics*, Vol. 32, No. 4, 2009, pp. 1077–1088.

[5] Linares, R., Crassidis, J. L., and Cheng, Y., "Constrained Relative Attitude Determination for Two-Vehicle Formations," *Journal of Guidance, Control, And Dynamics*, Vol. 34, No. 2, 2011, pp. 543–553.

[6] Vicon Motion Systems Limited, *Vicon MX Hardware System Reference*, 1st ed., 2007.

[7] Shuster, M. D. and Oh, S. D., "Three-Axis Attitude Determination from Vector Observations," *Journal of Guidance and Control*, Vol. 4, No. 1, Jan.-Feb. 1981, pp. 70–77.

[8] Cheng, Y., Crassidis, J. L., and Markley, F. L., "Attitude Estimation for Large Field-of-View Sensors," *The Journal of the Astronautical Sciences*, Vol. 54, No. 3/4, July-Dec. 2006, pp. 433–448.

[9] Shuster, M. D., "Kalman Filtering of Spacecraft Attitude and the QUEST Model," *Journal of the Astronautical Sciences*, Vol. 38, No. 3, July-Sept. 1990, pp. 377–393.

[10] Junkins, J. L., Hughes, D. C., Wazni, K. P., Pariyapong, V., and Kehtarnavaz, N., "Vision-Based Navigation for Rendezvous, Docking and Proximity Operations," *AAS Paper 99-021*, Vol. 52, Feb. 1999.

[11] Gunnam, K. K., Hughes, D. C., Junkins, J. L., and Kehtarnavaz, N., "A Vision-Based DSP Embedded Navigation Sensor," *IEEE Sensors Journal*, Vol. 2, No. 5, Oct. 2002, pp. 428–442.

[12] Andrle, M., Hyun, B., Crassidis, J. L., and Linares, R., "Deterministic Relative Attitude Determination of Formation Flying Spacecraft," *AIAA Guidance, Navigation, and Control Conference*, Honolulu, HI, Aug. 2008, AIAA-2008-6934.

[13] Shuster, M. D., "Deterministic Three-Axis Attitude Determination," *Journal of the Astronautical Sciences*, Vol. 52, No. 3, July-Sept. 2004, pp. 405–419.

[14] Bar-Shalom, Y., "On the Track-to-Track Correlation Problem," *IEEE Trans.on Automatic Control*, Vol. 26, No. 2, April 1981, pp. 571–572.